Pore Formation during Laser Beam Welding of Die-Cast Magnesium Alloy AM60B — Mechanism and Remedy

Controlled remelting of the fusion zone led to removal of gas bubbles, reducing porosity

BY H. ZHAO AND T. DEBROY

ABSTRACT. Weld metal porosity is a major concern during laser beam welding of magnesium alloys. This study seeks to identify both the mechanism of pore formation and a remedy for this problem during continuous-wave Nd:YAG laser beam welding of die-cast magnesium alloy AM60B. Preexisting pores in the base metal coalesced and expanded during welding of this alloy and, as a result, large pores were commonly present in the weld metal. Unlike laser beam welding of aluminum alloys, the stability of the keyhole was not a major factor in pore formation during laser beam welding of alloy AM60B. The porosity in the fusion zone increased with the increase in heat input, *i.e.*, increase in the laser power and decrease in the welding speed. It was found that well-controlled remelting of the fusion zone led to removal of gas bubbles and reduced porosity in the fusion zone.

Introduction

Magnesium and aluminum alloys are finding increased use in the automotive industry because of their excellent specific strength, good elongation and toughness. The specific strength, *i.e.*, the ratio of tensile strength and specific gravity, of die-cast magnesium alloy AM60B, 122 MPa, far exceeds that of low-carbon steel, which is 45 MPa. The use of these lightweight alloys can help automakers improve fuel economy and reduce greenhouse gas emissions. To make the most weight and cost savings in the use of automotive alloys, tailor-welded blanks are widely used in the auto body. Laser beam welding is a preferred method in the manufacture of tailor-welded blanks due to its high speed, low heat input and low weldment distortion. Increasing the use of aluminum and magnesium alloys in tailor-welded blanks will require improved technology to fabricate structurally sound and defect-free welds easily and reproducibly.

One of the major concerns during welding of magnesium and aluminum alloys is the presence of porosity in the weld metal that can deteriorate mechanical properties, particularly tensile strength and elongation (Refs. 1–3). However, pore formation during welding of magnesium alloys has not been systematically studied. In contrast, the mechanism of porosity formation during welding of aluminum alloys has received considerable attention (Refs. 4–12). Pore formation has been attributed to hydrogen rejection from the solid phase during solidification (Refs. 4–7) and imperfect collapse of the keyhole (Refs. 7–10). In addition, turbulent flow in the weld pool (Ref. 11) has also been linked with porosity formation. However, in a recent study, Pastor, *et al.* (Ref. 12), found keyhole stability played a major role in porosity formation during continuous-wave Nd:YAG laser beam welding of aluminum alloys 5182 and 5754. Furthermore, they showed segregation of hydrogen played an insignificant role in the formation of large pores in the welds.

Although the mechanism of pore formation during welding of aluminum alloys is better understood than magnesium alloys, there are some similarities between the welding of these two types of alloys. Both aluminum and magnesium have significantly higher hydrogen solubility in liquid than in solid. For magnesium, this difference in the hydrogen solubility can be observed from Fig. 1 (Ref. 13). Mikucki and Shearouse (Ref. 14) found the amount of porosity in the solidified magnesium alloy AZ91 was proportional to the dissolved hydrogen in the alloy. They also found that the rejection of hydrogen from the $Mg_{17}Al_{12}$ intermetallic compound assisted in the nucleation and/or growth of microporosity during the last stages of solidification of alloy AZ91 (Ref. 15). The difference in the solubility between the solid and liquid phases and the results of previous solidification studies (Refs. 14, 15) indicate hydrogen rejection needs to be considered as a possible cause of porosity formation during solidification of magnesium alloys (Refs. 14, 15).

Haferkamp, *et al.* (Ref. 16), observed more porosity in the fusion zone of non-vacuum die-cast alloy AM60B than vacuum die-cast alloy AZ91D, which had less gas inclusions in the base metal.

H. ZHAO and T. DEBROY are with the Department of Materials Science and Engineering, The Pennsylvania State University, University Park, Pa.

KEY WORDS

Magnesium Alloys
Porosity
Lasers
Laser Beam Welding
Die-Cast Magnesium
Automotive

They found for the same porosity level in welds, large pores are more detrimental to strength than small pores. The presence of gas inclusions in the base metal was thought to be an important factor in contributing to the formation of large pores during Nd:YAG laser welding of magnesium alloys (Ref. 16).

This research seeks to achieve both better understanding of pore formation in the AM60B fusion zone during laser beam welding and alleviation of the porosity problem for wider application of this alloy in the automotive industry.

Experimental Procedure

Bead-on-plate autogenous welds were produced on 2- to 6-mm-thick plates of die-cast magnesium alloy AM60B (Mg-5.2%Al) using a 3.0-kW, continuous-wave Nd:YAG laser. The base metal, alloy AM60B, contained 1.8 to 5 area-percent porosity, depending on plate thickness. The laser beam was delivered using a 600-μm-diameter fiber of fused silica to an f2 focus lens. A robot was employed to manipulate the motion of the lens assembly relative to the workpiece mounted horizontally on a stage. Prior to welding, the samples were ground with 400-grit grind cloth and then cleaned with acetone. The variables used were laser power in the range of 1.0 to 3.0 kW, welding speed between 125 and 300 in./min (53 to 127 mm/s) and beam defocusing in the range of –3.5 to 3.0 mm. A nomenclature of positive defocusing to indicate the focal point of the laser beam above the top surface of the workpiece and negative defocusing to represent the focal point below the top surface is used throughout this paper. A cylindrical copper nozzle having an inside diameter of 8.0 mm was utilized to provide helium as the shielding gas at a flow rate of 200 ft^3/h (5.7 m^3/h). Some specimens were rewelded to study the effect of remelting on fusion zone porosity.

The area-percent porosity, pore size distribution, and average pore radius in the base metal and fusion zone were measured by optical microscopy and computer image analysis using Image Pro® software. Based on the observed morphology and distribution of the pores in several cross sections, it was assumed the pores were spherical and evenly distributed. Therefore, the values of average pore radii for 3-D spherical pores were calculated by multiplying the average radii measured in 2-D cross sections by $\pi/2$ based on Fullman's theory (Ref. 17) for a polydispersed system of spheres. Unless otherwise specified, all the data of pore radii in this paper are 3-D pore radii. The number of pores per unit volume was calculated from the average pore radius and the volume-percent porosity, which is equal to the measured area-percent porosity.

Results and Discussion

Enhanced Porosity Due to Melting of the Base Metal

During welding of alloy AM60B it became clear the area-percent porosity in the fusion zone was often higher than that in the base metal that contained preexisting pores. Therefore, the origin of the enhanced porosity level in the fusion zone is an important question in this study. To answer this question fully, it is intuitive to consider the mechanisms of porosity formation in the welding of other nonferrous alloys. For example, during continuous-wave laser welding of automotive aluminum alloys, a significant number of large pores was formed in the fusion zone (Ref. 12). The pore formation was found to result from the instability of the keyhole. Therefore, the role of keyhole instability in the formation of large pores in the welding of alloy AM60B needs to be investigated together with other possible causes of porosity enhancement resulting from the coalescence and expansion of preexisting pores.

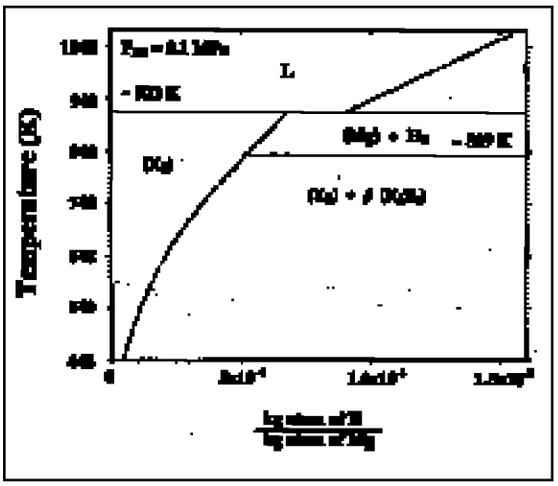

Fig. 1 — Solubility of hydrogen in magnesium (Ref. 13).

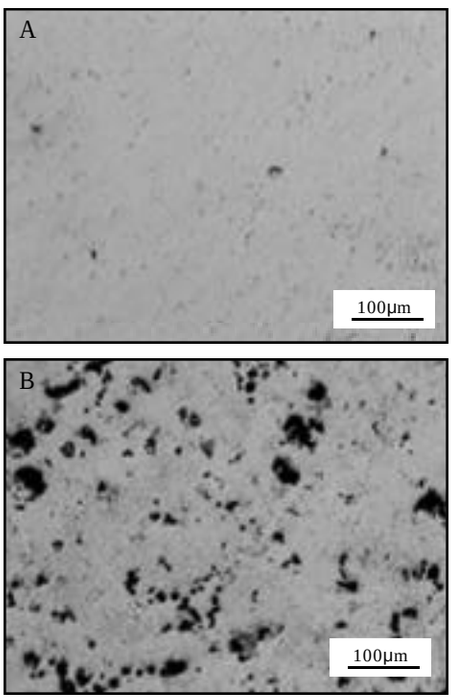

Fig. 2 — Micrographs showing features of porosity on unetched samples of 2-mm-thick alloy AM60B plates both before and after heat treatment at 863 K. A — Base metal before heat treatment; B — holding for 2 h.

Melting of the base metal can serve as a control experiment where the coalescence of the pores can be studied in the absence of any keyhole formation. The solidus and liquidus temperatures of alloy AM60B are 813 and 888 K, respectively. A few samples of the base metal were partially melted at 863 K and held for 2 h to study coalescence of pores. In this system, the changes in porosity can be attributed to heating, melting and pore coalescence while reducing the escape of gases that may occur easily from a fully melted alloy. Figure 2 shows the extent of porosity in the base metal and solidified sample after 2 h of heating at 863 K. Quantitative microscopy showed heating resulted in an increase in the average pore radius from about 2 to 6 mm, a decrease in number density from about 3400 to about 1500 per mm^2, and an increase in area-percent porosity from about 1.8% to about 7.0%. In short, the control experiment showed partial melting of the alloy resulted in significant increase in pore size and, more important, higher area-percent porosity than the base metal.

The increase in pore size and decrease in pore number density can be readily attributed to pore coalescence. However, coalescence alone cannot explain the increase in area-percent porosity observed in the partially melted and solidified samples. The thermal expan-

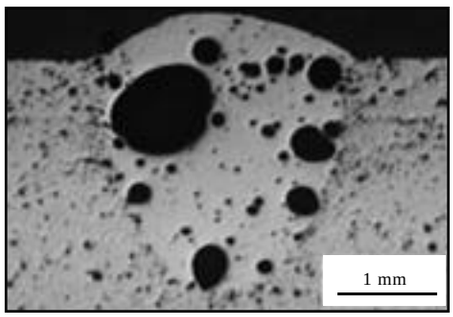

Fig. 3 — Pores observed in weld pool of laser beam welded alloy AM60B. Plate thickness 6 mm, laser power 1.5 kW, welding speed 250 in./min (106 mm/s), beam defocusing +1.0 mm, and shielding gas flow rate 200 ft³/h (5.7 m³/h) of helium.

sion of gas in the pores also has to be considered to understand the enhanced porosity in the heated metal as discussed later in this paper.

Enhanced Porosity in Welded Metal

It is observed from Fig. 3 that many large pores were formed in the fusion zone during laser welding of alloy AM60B. These pores are much larger than the preexisting pores in the base metal shown in Fig. 2A. Figure 4 shows many large pores are connected with the preexisting smaller pores in the base metal through one or more channels. For example, Fig. 4A shows a pore near the center of the picture was expanding by infusion of gas from the small preexisting pores in the base metal. Figure 4B shows a large pore was formed from the coalescence of several preexisting pores. Similarly, Figs. 4C and 4D show large pores in the fusion zone grew from the expansion and coalescence of small preexisting pores. The elongated shapes of these pores indicate they were expanding from the fusion boundary into the fusion zone. The proximity and connections between the large and the small pores and the shape of the large pores in Fig. 4 reveal the growth of the pores resulted from the coalescence and expansion of the preexisting pores in the base metal near the fusion boundary.

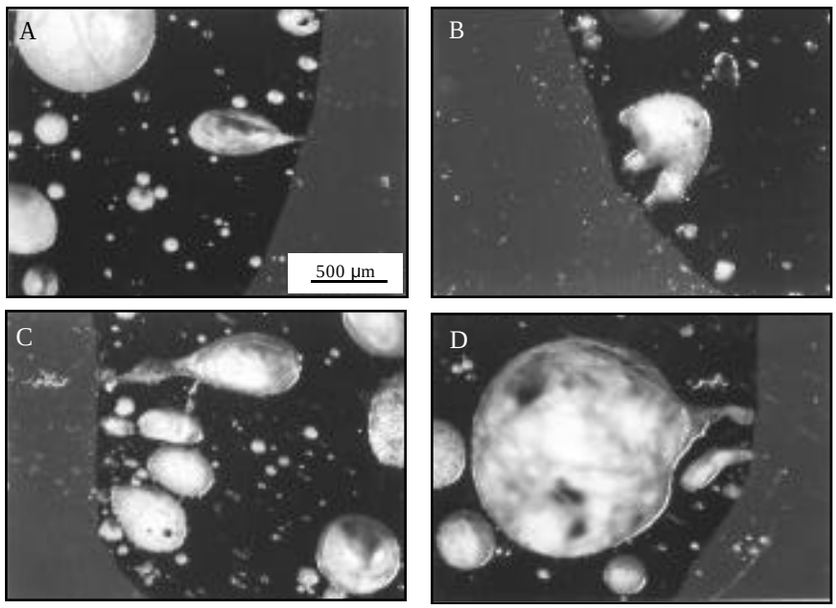

Fig. 4 — Formation of large pores in the fusion zone (the black region) due to the expansion and coalescence of the preexisting pores in the base metal (the gray region) of alloy AM60B. All figures have the same magnification as shown in A.

Table 1 — Pore Number Density, Average Pore Radius, and Area Percent Porosity in the Base Metal and Weld Metal of 2-mm-Thick Alloy AM60B Plates

	Base Metal	Weld Metal					
Welding Speed (mm/s)		53	64	74	85	95	106
Measured number of pores per unit area (mm^{-2})	3.4×10^3	51	33	52	43	43	51
Number of pores per unit volume (mm^{-3})	5.37×10^5	223	119	293	199	193	280
Measured average 2-D pore radius (μm)	1.3	43.7	52.8	37.1	42.0	42.4	36.0
Average 3-D pore radius (μm)	2.0	68.6	82.9	58.3	65.9	66.6	56.5
Estimated average 3-D pore radius (μm)		66.5	82.7	60.4	69.2	69.9	61.4
Measured area percent porosity	1.8	30.7	28.6	22.7	24.0	24.3	20.6
Estimated area percent porosity		27.5	28.2	27.1	27.6	27.6	27.1

Welding conditions: laser 1.5 kW, focused beam, shielding gas flow rate 200 ft³/h (5.7 m³h) of helium, and various welding speeds.

Pore Coalescence and Expansion

Figure 5 shows the typical number densities of pores of various sizes in the base metal and weld metal. It is observed that the pore radii in the fusion zone are more than one order of magnitude larger than those in the base metal, while the pore number densities in the weld metal are nearly two orders of magnitude smaller. The reduction in the number of pores per unit area of fusion zone indicates significant coalescence of the preexisting pores during welding. The average pore radius, number density and area-percent porosity measured in the base metal and weld metal for different welding speeds are given in Table 1. It is observed that the area-percent porosity in the weld metal was about 11 to 17 times that in the base metal depending on welding speed.

To understand the increase in area-percent porosity in the weld metal, pore expansion due to coalescence of the preexisting pores needs to be considered. When the base metal is melted, pressure in the pores tends to equal the sum of the surface tension pressure and the pressure in the surrounding liquid. Since surface tension pressure decreases with an increase in pore radius and the pressure in the surrounding liquid is almost constant, the pressure inside a small pore is larger than that in a large pore. If several small pores coalesce to form a large pore, there

will be a net increase in total pore volume due to both coalescence and reduction of surface tension pressure. Furthermore, pores in the alloy can expand when they are heated to higher temperatures. Therefore, the thermal expansion of pores also needs to be considered. During welding, significant pore expansion occurs due to heating. However, during solidification, the pores shrink with the reduction in the temperature of the liquid metal. The shrinking continues until the solidus temperature is reached. Any further lowering of temperature reduces pore sizes by a much smaller amount. Thus, the net expansion due to temperature change is equivalent to heating the pores from room temperature to solidus temperature.

The average pore radius and area-percent porosity in the weld metal for different welding conditions were estimated considering pore coalescence and thermal expansion. The calculation procedure is described in the Appendix. Results in Table 1 show fair agreement was achieved between the measured and estimated values of average pore radius and area-percent porosity. The good agreement indicates the increase in weld metal porosity can be attributed to pore coalescence and thermal expansion during welding.

Keyhole Stability

In order to study the influence of keyhole stability on porosity formation, different laser beam power densities were used by changing the extent of beam defocusing during welding of alloy AM60B. The porosity in the fusion zone is plotted as a function of beam defocusing in Fig. 6. It is observed that the amount of porosity is not sensitive to beam defocusing. The welding mode gradually changed from keyhole to conduction mode as the extent of beam defocusing increased. The mixed mode of welding, characterized by the presence of two types of weld pool geometry typical of both conduction and keyhole modes in various cross sections of the same welded sample, was not observed in the welding of AM60B.

In contrast with the mode of welding for AM60B, three modes of welding were identified depending on the degree of beam defocusing in the welding of aluminum alloys 5182 and 5754 (Ref. 12). At a high degree of beam defocusing, beam power density was lower than the threshold value for keyhole formation, resulting in conduction mode welding and a shallow weld pool. When the beam was nearly focused, the power density was well above the threshold value to form a keyhole and a deep weld pool characteristic of the keyhole mode of welding formed. Porosity was rarely observed in either conduction or the keyhole mode of welding. However, when beam power density was just above the threshold value for keyhole formation, an unstable keyhole was formed that collapsed with any small disturbance. As a result, in various cross sections of the same welded sample, the weld pool shapes characteristic of either conduction or keyhole mode were observed. Porosity was formed primarily in this mixed mode of welding due to keyhole instability in the automotive aluminum alloys as shown in Fig. 7.

The absence of a mixed mode of welding during welding of magnesium alloy AM60B indicates the keyhole was more stable than the one for the welding of aluminum alloys. The stability of the keyhole depends on a balance between surface tension pressure and vapor pressure. Surface tension pressure tends to close the keyhole while vaporization tends to keep it open. Aluminum alloys have higher surface tension and much lower vapor pressure than magnesium alloys (Ref. 18). Therefore, it is easier to maintain a keyhole for the welding of magnesium alloys than aluminum alloys. Furthermore, vapor pressure in the keyhole during laser welding of alloys 5182 and 5754 was mainly due to magnesium in the alloys (Refs. 19, 20). Because of its low concentrations in these alloys, magnesium could be depleted from the keyhole surface, resulting in vapor pressure drop and, consequently, collapse of the keyhole. On the other hand, magnesium is the main constituent in alloy AM60B and vaporization of magnesium has little impact on the alloy composition. Therefore, the keyhole was more stable during

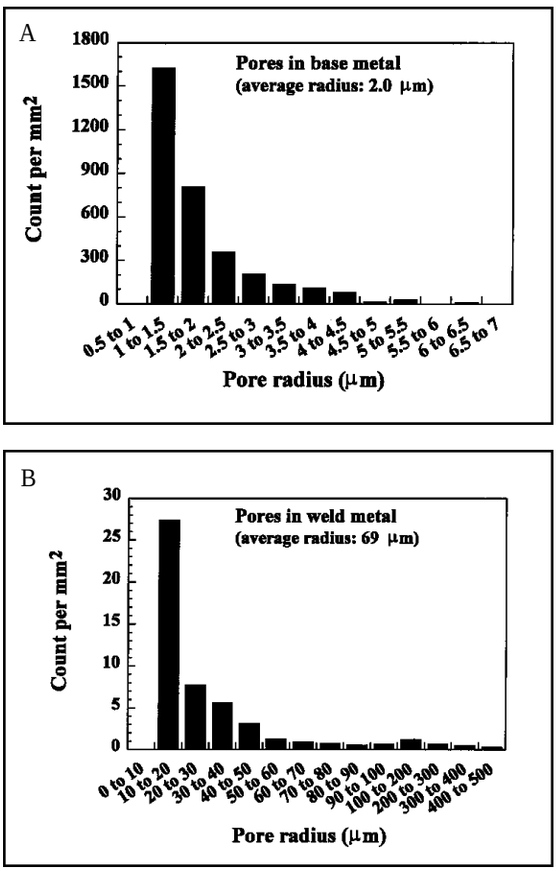

Fig. 5 — Pore size distributions. A — Base metal; B — fusion zone of laser-welded alloy AM60B using a focused beam. Plate thickness 2 mm, laser power 1.5 kW, welding speed 125 in./min (53 mm/s), and shielding gas flow rate 200 ft³/h (5.7 m³/h) of helium.

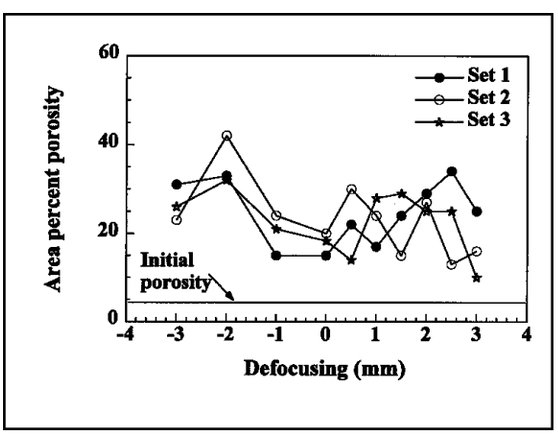

Fig. 6 — Porosity formed in laser welds of alloy AM60B at several beam defocusing values. Plate thickness 6 mm, laser power 1.5 kW, welding speed 250 in./min (106 mm/s), and shielding gas flow rate 200 ft³/h (5.7 m³/h) of helium.

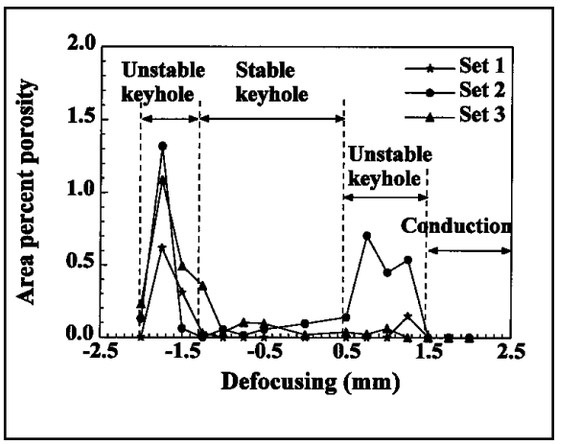

Fig. 7 — Porosity produced at several beam defocusing values in alloy 5754. Plate thickness 1.45 mm, laser power 3.0 kW, welding speed 150 in./min (64 mm/s), and shielding gas flow rate 200 ft³/h (5.7 m³/h) of helium (Ref. 12).

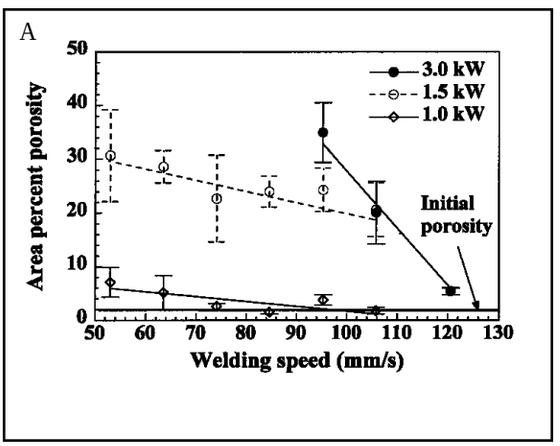

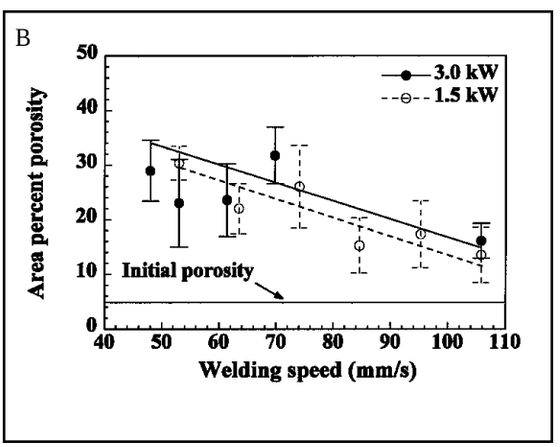

Fig. 8 — Porosity formed in laser welds of alloy AM60B plates, with thickness of (A) 2 mm and (B) 6 mm, for different welding speeds and laser powers using focused beam and shielding gas flow rate 200 ft³/h (5.7 m³/h) of helium.

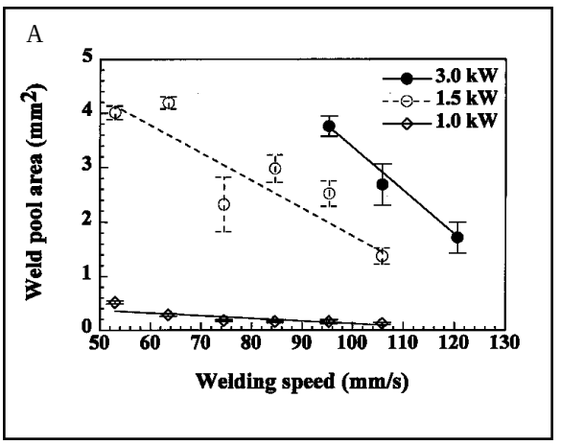

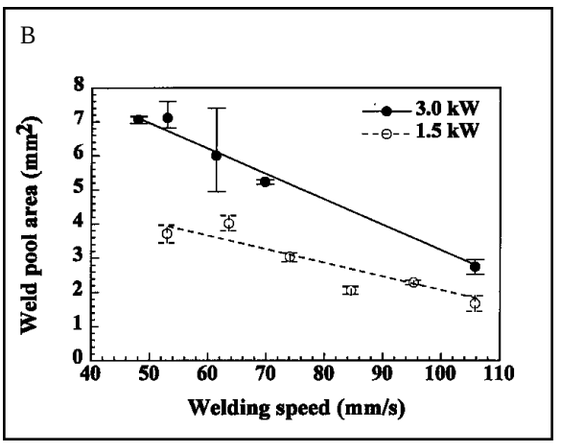

Fig. 9 — Weld pool area produced in laser welds of alloy AM60B plates, with thickness of (A) 2 mm and (B) 6 mm, for different welding speeds and laser powers using focused beam and shielding gas flow rate 200 ft³/h (5.7 m³/h) of helium.

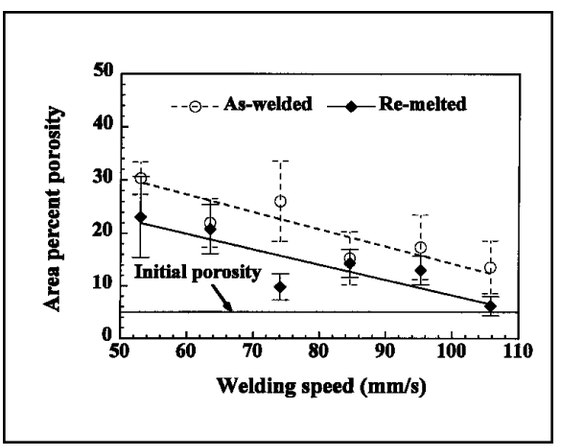

Fig. 10 — Area percent porosity produced on as-welded (single-run) and remelted (double-run) samples of alloy AM60B with a focused beam. Plate thickness 6 mm, laser power 1.5 kW for first run and 1.0 kW for second run, and shielding gas flow rate 200 ft³/h (5.7 m³/h) of helium.

laser beam welding of AM60B than during laser beam welding of aluminum alloys. The keyhole instability was not a problem in the pore formation during laser beam welding of alloy AM60B.

Reduction of Weld Metal Porosity

The area-percent porosity formed in the fusion zone for different welding conditions is shown in Fig. 8. The data show the porosity in the fusion zone was much higher than that in the base metal for most welding conditions used. It is also observed the porosity in the fusion zone decreased with decreasing heat input, *i.e.*, decreasing laser power and increasing welding speed. At low heat input, it was possible to obtain welds with porosity levels similar to that in the base metal. However, the weld pool cross-section area decreased with a decrease in heat input, especially with a decrease in laser power as shown in Fig. 9. For a given plate thickness, the heat input has to be higher than a certain level to obtain full penetration welding. Therefore, besides reducing heat input, a more practical method to alleviate the porosity problem has to be found. This issue is addressed in the following paragraph.

The transport of gas bubbles in a weld pool containing recirculating liquid metal is complex. During welding, gas bubbles drifted with the flow of liquid metal and at the same time had a tendency to float upward due to the difference in the densities of the bulk liquid and the bubbles. Furthermore, the vigorous flow of weld metal promoted coalescence of bubbles. It is fair to expect that due to the rapid thermal cycle, the pores formed in the fusion zone had little time to float out of the weld pool in a single welding thermal cycle. Therefore, small pores that require a long time for flotation could not be removed from the weld pool within the available time. If a second run of welding was performed, the pores in the fusion zone that are already much larger than the preexisting pores in the base metal might have a second chance to float out of the weld pool. Moreover, these pores could also coalesce to form even larger bubbles. Therefore, more significant flotation of these bubbles should take place during remelting of the fusion zone since larger bubbles are more easily separated by gravity.

Based on these considerations, a second run of welding was performed on some welded samples to examine the effect of remelting on porosity reduction. Figure 10 shows the area-percent porosity formed in the as-welded (single run) and remelted (double run) samples for different welding speeds. It is observed that remelting of the fusion zone significantly reduced porosity. Therefore, well-controlled remelting of the fusion zone by a second run of welding can reduce porosity by allowing some pores formed during the first run of welding to be removed. The keyhole mode of welding was obtained for both the first and second run of welding. The reduction of porosity in the remelted fusion zone also indicated porosity due to keyhole instability during welding was not significant and porosity formed in the fusion zone was due to the coalescence and expansion of preexisting pores in the base metal.

Summary and Conclusions

The mechanism of porosity formation during continuous-wave Nd:YAG laser beam welding of die cast magnesium alloy AM60B has been studied. A practical method to alleviate the porosity problem was sought based on the mechanistic understanding. The major findings are as follows:

1) Significant increase in volume percent of porosity was observed in the fusion zone for most of the welding conditions used. The coalescence and expansion of small preexisting pores due to heating and reduction of internal pressure contributed to the porosity increase in the fusion zone.

2) The stability of the keyhole was not a major factor in fusion zone pore formation during laser beam welding of alloy AM60B. The keyhole formed during welding of alloy AM60B was more stable than that formed in aluminum alloys 5182 and 5754.

3) The amount of porosity in the fusion zone decreased with a decrease in heat input, *i.e.*, decrease in laser power or increase in welding speed. Porosity levels similar to that in the base metal could be obtained when heat input was low.

4) Well-controlled remelting of the fusion zone allowed some of the pores to be removed, resulting in reduced porosity in the fusion zone. The reduction in porosity also indicates keyhole instability during laser beam welding of alloy AM60B was not important for pore formation.

Acknowledgment

The authors thank Dr. D. White of Ford Motor Co. for the donation of alloy AM60B used in this study. This research was funded by the U.S. Department of Energy (Grant Nos. DE-FG02-96ER45602 and DE-FG02-84ER45158). We thank Dr. S. A. David for his generous help in conducting the rewelding experiments.

References

1. Lawrence, F. V., Jr. 1973. WRC Bulletin 181: 1–23.

2. Ashton, R. F., and Wesley, R. P. 1975. *Welding Journal* 54(3): 95-s to 98-s.

3. Katoh, M. 1996. *Welding International* (UK) 10(10): 771–777.

4. Woods, R. A. 1974. *Hydrogen in Metals*, eds. I. M. Bernstein and A. W. Thompson, pp. 713–725. ASM International, Materials Park, Ohio.

5. Masahiro, U., and Satoru, O. 1974. *Trans. Nat. Res. Inst. Met.* 16(2): 67–74.

6. Kutsuna, M. 1993. *Welding in the World* IIW 31: 126–135.

7. Katayama, S. 1996. *Journal of Light Metal Welding and Construction* 34(4): 31–41.

8. Schauer, D. A., and Giedt, W. H. 1978. *Welding Journal* 57(7): 189-s to 195-s.

9. Whitaker, I. R., McCartney, D. G., and Steen, W. M. 1992. *ICALEO '92*: 565-573.

10. Matsunawa, A., Kim, J. D., Seto, N., Mizutani, M., and Katayama, S. 1998. *Journal of Laser Applications* 10(6): 247–254.

11. Kim, J. S., Watanabe, T., and Yoshida, Y. 1995. *Journal of Laser Applications* 7(1): 38–46.

12. Pastor, M., Zhao, H., Martukanitz, R. P., and DebRoy, T. 1999. *Welding Journal* 78(6): 207-s to 216-s.

13. Avedesian, M,. and Baker, H. 1999. *Magnesium and Magnesium Alloys*, ASM International, Materials Park, Ohio.

14. Mikucki, B. A. and Shearouse, J. D. III. 1993. *Proceedings of Magnesium Properties and Applications for Automobiles Conference*, Detroit, Mich., Society of Automotive Engineers, Inc., pp. 107–115.

15. Shearouse, J. D. III, and Mikucki, B. A. 1994. SAE Transactions. *Journal of Materials & Manufacturing*, Vol. 103, pp. 542–552.

16. Haferkamp, H., Bach, Fr.-W., Burmester, I., Kreutzburg, K., and Niemeyer, M. 1996. *Proceedings of the Third International Magnesium Conference*, Edited by Lorimer, G. W., pp. 89–98. The Institute of Materials, London, U.K.

17. Fullman, R. L. 1953. *Trans. AIME*, 197: 447–452.

18. Brandes, E. A. 1983. *Smithells Metals Reference Book*, 6th edition, London, Boston, Butterworth, in association with Fulmer Research Institute Ltd.

19. Block-Bolten, A., and Eagar, T. W. 1984. *Metallurgical Transactions* 15B: 461–469.

20. Zhao, H., and DebRoy, T. 2001. *Metallurgical and Materials Transactions* 32B: 163–172.

Appendix

Estimation of Pore Expansion during Welding

The pressure inside a stable bubble, P_i, is the sum of surface tension pressure, P_s, and pressure in the liquid, P_a, *i.e.*,

$$P_i = P_s + P_a \quad (1a)$$

The surface tension pressure is given by

$$P_s = 2\sigma/r \quad (2a)$$

where σ and r are the surface tension and pore radius, respectively, and the pressure in the liquid consists of the ambient pressure and a small hydrostatic head.

Consider that N number of small spherical bubbles of radius r_0 are heated from temperature T_0 to temperature T and then these pores coalesce to form a single large spherical bubble of radius r. Assuming the pores are stable before and after heating and coalescence, and considering for simplicity a constant surface tension, σ, the pressure inside the small bubbles is given by

$$P_0 = 2\sigma/r_0 + P_a \quad (3a)$$

And the pressure inside the large bubble is given by

$$P = 2\sigma/r + P_a \quad (4a)$$

According to ideal gas law, we have

$$nRT_0 = P_0V_0 = (4/3)\pi N(2\sigma/r_0 + P_a)r_0^3 \quad (5a)$$

$$nRT = PV = (4/3)\pi(2\sigma/r + P_a)r^3 \quad (6a)$$

where n is the total number of moles of gas in the bubbles, R is the gas constant, and V_0 and V are the total volumes of the bubbles before and after the heating and coalescence, respectively. Combining Equations 5a and 6a, we obtain

$$(2\sigma/r + P_a)r^3 = (T/T_0)N(2\sigma/r_0 + P_a)r_0^3 \quad (7a)$$

The radius r of the large bubble can be calculated from Equation 7a from known values of σ, P_a, T, T_0, N, and r_0. The ratio of volumes after and before the heating and coalescence is given by

$$V/V_0 = r^3/(Nr_0^3) \quad (8a)$$

Let us consider the coalescence of preexisting pores in the weld metal obtained using laser power of 1.5 kW and welding speed of 53 mm/s. As shown in Table 1, in the base metal, the average radius of the preexisting pores is 2.0 μm, the pore number density is 5.37 x 10^5 per mm^3, and area percent porosity is 1.8. In the weld metal, the pore number density is 223 per mm^3. Therefore, on average, about 2408 of preexisting pores in the base metal coalesced to form one large pore in the weld metal. During welding, the weld metal was first heated to very high temperatures and the pores in the metal expanded significantly. During the subsequent cooling process, the pores shrank with the reduction in the temperature of the liquid metal until the solidus temperature was reached. Thus, the net expansion due to the temperature is equivalent to heating the pores from room temperature (298 K) to the solidus temperature of 813 K for alloy AM60B. Therefore, taking N = 2408, r_0 = 2.0 μm, T_0 = 298 K, T = 813 K, P_a = 1.013 x 10^5 P_a, and σ = 0.56 Nm^{-1}, we can solve Equation 7a and obtain the average radius of the resulting large pores in the weld metal to be r = 66.5 μm. The ratio of total volume of pores in the weld metal and that in the base metal is calculated by

$$V/V_0 = r^3/(Nr_0^3) = 66.5^3/(2408 \times 2.0^3) \approx 15.3$$

Since the area-percent porosity is equal to volume-percent porosity, the area-percent porosity in the weld metal will be estimated to be 1.8 x 15.3 = 27.5. Similar calculations were done for other welding conditions to estimate the area-percent porosity in the weld metal and the results are shown in Table 1. It is observed that the estimated values of average pore radius and area-percent porosity in the weld metal fairly agree with the measured values. The good agreement indicates the increase in porosity in the weld metal can be attributed to pore coalescence and thermal expansion during welding.